Available online at www.sciencedirect.com
SCIENCE DIRECT®
Composites Science and Technology 63 (2003) 1911–1920
COMPOSITES SCIENCE AND TECHNOLOGY
www.elsevier.com/locate/compscitech

High performance estimations of delamination of graphite/epoxy laminates with electric resistance change method

Akira Todoroki*, Miho Tanaka[1], Yoshinobu Shimamura

Department of Mechanical Sciences, and Engineering, Tokyo Institute of Technology, 2-12-1, O-okayama, Meguro, Tokyo 1528552, Japan

Received 6 January 2002; received in revised form 15 December 2002; accepted 20 March 2003

Abstract

Delamination of laminated composites is usually invisible or difficult to detect visually. Delamination causes low reliability for primary structures. Automatic systems for in-service delamination identifications are desired to improve low reliability. The present study employs an electric resistance change method for delamination detection. Since the method adopts reinforcement carbon fiber itself as sensors for delamination detection, this method does not reduce static or fatigue strength; also, the method is applicable to existing structures. Authors have found that the electric resistance change method with response surfaces is very effective experimentally and analytically. However, a large error of estimation remains for estimation of delamination location. In the present study, a new data processing procedure is proposed to improve performance of estimations of delamination location. The new method is applied to laminated composite beams. A delamination crack of a laminated composite beam is monitored with the new method using FEM analyses. As a result, the method reveals excellent performance of estimations of delamination location even for new data not used in regression equations.

Keywords: A. Polymer-matrix composites; A. Smart materials; B. Electrical properties; C. Delamination; Electric resistance

1. Introduction

The electric resistance change method has been employed recently by many researchers to identify internal damage such as delaminations and matrix cracks in carbon fiber reinforced plastics (CFRP) laminates [1–18]. In contrast to fiber-optic sensors, the electric resistance change method does not require expensive instruments for measurement. Since the method adopts reinforcement carbon fiber itself as sensors for damage identifications, this method does not cause reduction of static strength or fatigue strength; it is applicable to existing structures merely by attachment of multiple electrodes.

The authors have investigated applicability of the electrical resistance change method through experimentation; delamination crack length was measured for edge cracks from delamination-resistance tests [19,20]. However, delamination cracks are usually embedded cracks for practical composite structures. Embedded cracks of beam type specimens were also detected experimentally by Todoroki using the electric resistance change method with graphite/PEEK composites [21]. Several FEM analyses have also elucidated the effect of orthotropic electrical resistance on delamination monitoring of cross-ply laminates [22,23]. Beam type specimens were employed to monitor delamination creations experimentally [24]; plate type specimens of cross-ply laminates and quasi-isotropic laminates were also adopted to monitor delamination creation experimentally [25,26].

For these studies, a response surface method was adopted as a tool to solve inverse problems: delamination location and size were obtained from measured electric resistance changes of multiple segments between electrodes. In this method, performance of estimations of delamination location was inadequate compared with delamination size estimations; also, it was necessary to improve estimation performance, especially for small delaminations [24,27].

In light of those difficulties, the present study uses many FEM analyses of various delamination sizes and

* Corresponding author. Tel./Fax: +81-3-5734-3178.
E-mail address: atodorok@ginza.mes.titech.ac.jp (A. Todoroki).
[1] Graduate student of Tokyo Institute of Technology.

0266-3538/03/$ - see front matter © 2003 Elsevier Ltd. All rights reserved.
doi:10.1016/S0266-3538(03)00157-X

locations of beam type specimens to investigate large errors of estimation of delamination locations; furthermore an improvement to obtain higher estimation performance is proposed for the data processing method before making response surfaces. This new method is applied to estimate delamination location and size of beam type specimens; performance of the new estimation method is evaluated analytically herein.

2. Electric resistance change method for delamination monitoring

Graphite fiber has high electric conductivity; the epoxy matrix is its insulator. For ideal graphite/plastic composites, electric conductivity in the fiber direction is high. Ideal conductivity can be calculated easily by multiplying the fiber volume fraction to electric conductivity of graphite fiber. On the other hand, electric conductivity in the transverse direction vanishes for ideal, straightly aligned fibers.

Practical graphite fiber in a unidirectional ply is not straight, as shown in Fig. 1(a). The curved graphite fibers contact one another, comprising a graphite-fiber network within a ply. The contact-network brings non-zero electric conductivity even in the transverse direction. In the same way, the fiber-network produces non-zero electric conductivity in the thickness direction in a ply. Electric conductivity in the transverse direction is much lower than that in the fiber direction. Abry et al. [11] and the authors [26] found experimentally that the electric conductivity ratio of the transverse direction (σ_{90}) to the fiber direction (σ_0) is very small, and that the electric conductivity ratio of the thickness direction (σ_t) to the fiber direction is smaller than that of the transverse direction. The example of the case of fiber volume fraction is 62% is shown in Table 1. The result indicates that graphite/epoxy laminates have significantly strong orthotropic electric conductance.

Although fiber-network structure in the thickness direction is almost identical to the structure of the transverse direction in a ply, through-the-thickness

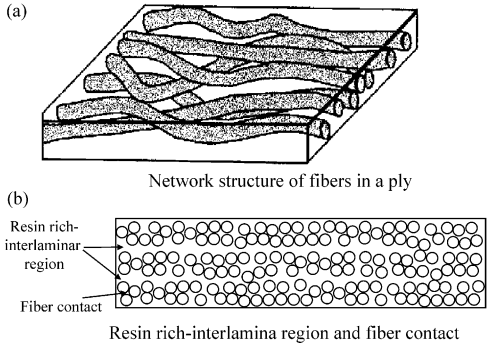

Fig. 1. Schema of practical structure of graphite/epoxy composite.

Table 1
Material properties of graphite/epoxy composites employed here

V_f	σ_0 $(\Omega m)^{-1}$	σ_{90}/σ_0	σ_t/σ_0
062	5500	3.71×10^{2}	3.77×10^{-3}

conductivity σ_t is smaller than the σ_{90} for normal laminates. That is because thin electrically insulating resin-rich interlamina exist there. For ideal graphite/epoxy composites, σ_t vanishes due to the resin-rich interlamina. For practical graphite/plastics composites, however, prepreg plies are serpentine as the fibers in a ply shown in Fig. 1(b). The ply curvature induces fiber contact through plies and causes non-zero electric conductance in the thickness direction even for thick laminated graphite/epoxy laminates. Contact among plies causes non-zero electric conductance in the thickness direction. Thus, the σ_{90} is usually larger than the σ_t. When a crack grows in the interlamina, the crack breaks the fiber-contact-network between plies. Breakage of the contact network causes increased electrical resistance of graphite/epoxy composites. Therefore, delamination cracks can be detected by electric resistance change of graphite/epoxy composite laminates.

Fig. 2 shows a schematic representation of the delamination-monitoring system proposed by the authors. Multiple electrodes are mounted on the specimen surface as shown in Fig. 2. All these electrodes are placed on a single side of the specimen. Usually, it is impossible to place electrodes and lead wires outside of aircraft structures. Location of electrodes on the single side surface is a model of placing electrodes in a thin shell aircraft structure. The authors have performed several FEM analyses and concluded that electric current should be charged in the fiber direction of the surface ply to monitor a delamination crack [26]. Electric-resistance change of each segment between electrodes is measured with a conventional electric resistance bridge circuit as shown in Fig. 3. Electric resistance changes among all segments are measured for various delamination sizes and locations. Using measured data, relations between electric resistance change and delaminations (location and size of delaminations) are obtained using response surfaces. The response surface method is employed here since some authors have revealed that response surfaces are better than artificial neural networks for this inverse problem [28]. After calculations of response surfaces, delamination location and size can be estimated with response surfaces from measured electric-resistance changes.

In the case shown in Fig. 2, four electric resistance changes are measured at four segments (obtained electric resistance change: e_1, e_2, e_3, and e_4). Many experiments or calculations must be performed to create response surfaces. Many data sets of delamination

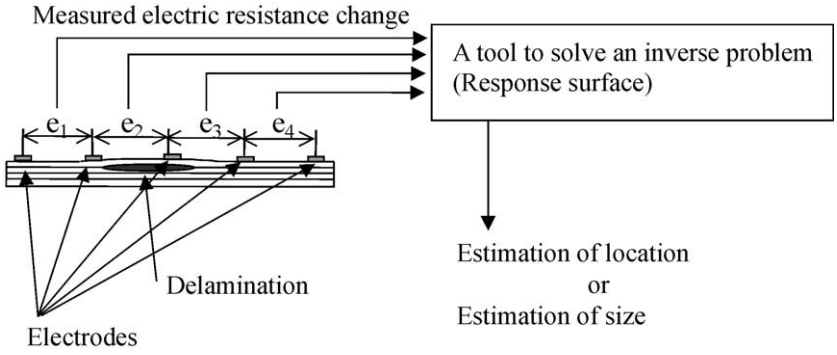

Fig. 2. Schematic representation of delamination identification method using electric resistance change method with a response surface.

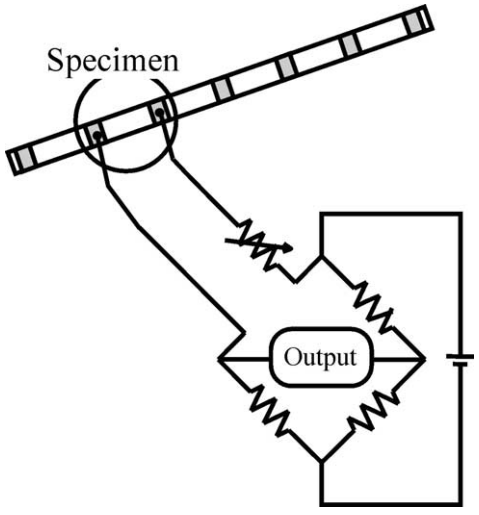

Fig. 3. Electric resistance bridge circuit for measuring electric resistance change.

location, size and electric resistance changes are obtained from experiments. In cases of quadratic polynomials, response surfaces estimating delamination location (x) and size (a) are as follows.

$$x = \beta_0^x + \beta_1^x e_1 + \beta_2^x e_2 + \beta_3^x e_3 + \beta_4^x e_4 + \beta_5^x e_1^2 + \beta_6^x e_2^2 + \beta_7^x e_3^2 + \beta_8^x e_4^2 + \beta_9^x e_1 e_2 + \beta_{10}^x e_1 e_3 + \beta_{11}^x e_1 e_4 + \beta_{12}^x e_2 e_3 + \beta_{13}^x e_2 e_4 + \beta_{14}^x e_3 e_4 \quad (1)$$

$$a = \beta_0^a + \beta_1^a e_1 + \beta_2^a e_2 + \beta_3^a e_3 + \beta_4^a e_4 + \beta_5^a e_1^2 + \beta_6^a e_2^2 + \beta_7^a e_3^2 + \beta_8^a e_4^2 + \beta_9^a e_1 e_2 + \beta_{10}^a e_1 e_3 + \beta_{11}^a e_1 e_4 + \beta_{12}^a e_2 e_3 + \beta_{13}^a e_2 e_4 + \beta_{14}^a e_3 e_4 \quad (2)$$

where all coefficients (β_i^x and β_i^a, $i = 1 \ldots 14$) are obtained with the least square error method [29]. Lack of fit is evaluated with the adjusted coefficient of multiple determination R^2_{adj} [29]; R^2_{adj} is defined as

$$R^2_{adj} = 1 - \frac{SS_E/(n-k-1)}{S_{yy}/(n-1)}, \quad (3)$$

where SS_E is the square sum of errors, S_{yy} is the total sum of squares, n is the number of data sets, and k is the number of unknown coefficients. The value of R^2_{adj} is equal to or lower than 1.0. Higher values of R^2_{adj} imply good fit. When the response surface shows very good fit, R^2_{adj} approaches 1.0.

3. FEM analysis

In the present study, FEM analyses are employed for investigations. Beam type specimens were adopted for FEM analyses of delamination monitoring as shown in Fig. 4. Beam length is 210 mm and beam thickness is 2 mm. Seven 5-mm wide electrodes are mounted on the specimen surface; spacing of electrodes is 35 mm. Stacking sequence of the specimen is [0/90]s. In this study, ply thickness is fixed at 0.5 mm, four times larger than the normal prepreg.

The authors have performed delamination monitoring for identification of delamination size and location using the electric resistance change method [19–27]. In this method, multiple electrodes are mounted on the laminate surface; then, electric resistance change is measured after creation of a delamination in each segment between electrodes. Consider the case of a five-electrode-beam specimen as shown in Fig. 2. In this case, five electrodes are mounted on the specimen top surface. Consequently, the specimen has four segments between electrodes; electric resistance changes of the four segments are measured after creation of a delamination. A large number of data sets of electric resistance changes are collected; these sets of data are used for showing a relationship between measured electric resistance changes and the delamination crack. Since it is an inverse problem to obtain delamination location and size from the measured set of electric resistance changes, authors have adopted artificial neural networks and

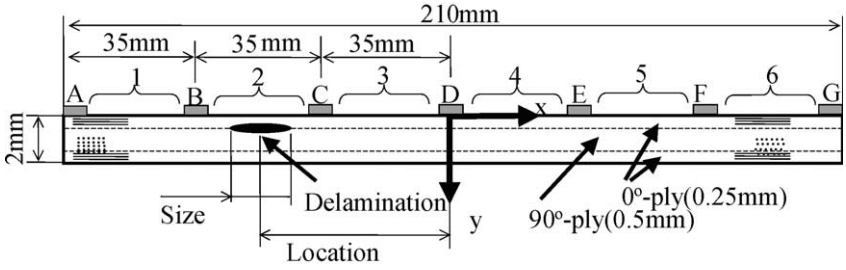

Fig. 4. Specimen configuration and size. Stacking sequence: [0/90]s.

response surfaces to obtain the relationship [28]. Using this relationship, delamination location and size (length) can be monitored successfully [24,25,28]. The reason why all electrodes are mounted on the specimen top is to simulate internal monitoring of thin-shell type structures such as aerospace structures.

Since the diameter of a typical graphite fiber is much smaller than the size of FEM elements adopted here, the inhomogeneous orthotropic graphite/epoxy composite material is assumed to be a homogeneous orthotropic material for present FEM analysis. In the thickness direction, however, thickness of the resin rich layer, which causes lower electric conductance compared to that of the transverse direction, is smaller than ply thickness. This introduces the difficulty of modeling electric conductance in the thickness direction. In the present study, four-node-rectangular elements are adopted for analysis; each element is approximately 0.125 mm×0.125 mm. Since ply thickness is 0.5 mm, a ply comprises four elements in the thickness direction. This implies that average electric conductance in the thickness direction in a ply can be obtained by assuming homogeneous electric conductance in the thickness direction. Therefore, electric conductance in the thickness direction is treated as approximately homogeneous here.

The FEM analyses are performed using a commercially available FEM tool named ANSYS. Using the ANSYS auto mesh generation system, the specimen model is divided into approximately 28,160 two-dimensional elements. A delamination crack is usually made near the surface; it is located opposite to the impacted surface. To simulate this delamination location, a delamination crack should be made at the interface near the inside surface. In this study, the outside surface is the bottom surface and the inside surface is the top surface, as in Fig. 2. Therefore, a delamination crack is made at the interface between the top 0° ply and the middle 90° ply, as shown in Fig. 2. On delamination crack surface lines, all nodes are doubly defined to represent delamination crack surfaces. When a delamination crack is created, doubly defined nodes on delamination crack surfaces are released with each other to represent electric current insulation. For a delamination crack induced in the FEM model, the present study subsumes that the crack mouth is fully opened after delamination, although an actual delamination crack has crack surface contact. This simplifies the FEM model; the effect of this model must be investigated experimentally. Such experimental investigation will occupy our future work.

Table 1 shows electric conductivity used for FEM analysis. To compute electric resistance changes, direct electric current of 30 mA is charged from one electrode; also, electric voltage of the other side of the segment is set to 0 V. After computation, electric voltage at the electrode is divided by electric current (30 mA) to calculate electrical resistance of the segment. After this computation, a delamination is created and similar computation is conducted to obtain electric resistance changes at the segment. In the present study, since the total number of electrodes is seven, the total number of segments is six as shown in Fig. 4.

Definitions of delamination size and location are also shown in Fig. 4. Delamination size is defined as the length of the delamination crack and delamination location is defined as the location of the center of the delamination crack from the middle of the specimen. Delamination location in the thickness direction is ignored in the present study because the laminate is thin.

Various types of delaminations are computed to obtain electric resistance changes. The total number of analyses is 193. Five types of length of delamination are computed: those are 2, 10, 20, 30, and 40 mm. To confirm performance of estimations for new data that are not used for regressions, six other delamination types are computed; those are: 1, 5, 15, 25, 35, and 45 mm.

4. Results of the previous identification method

A response surface to estimate delamination locations is made from 193 data sets of FEM analyses using a quadratic polynomial. Fig. 5 shows those results. The abscissa is the given delamination location; the ordinate is the estimated delamination location. Plotted symbols on the diagonal line indicate that estimations are exact. As shown in Fig. 5, most symbols are scattered; also, the adjusted coefficient of multiple-determination R^2_{adj} is

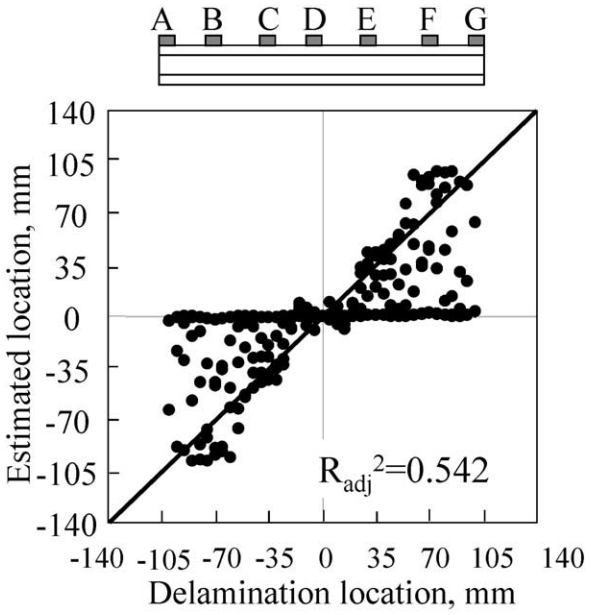

Fig. 5. Estimations of delamination location using a response surface

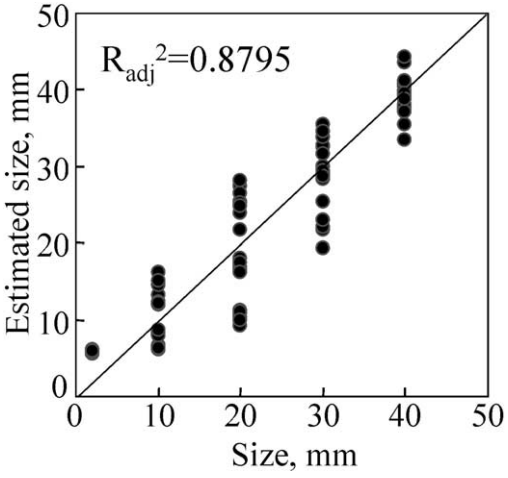

Fig. 6. Estimations of delamination size using a response surface created from obtained data (number of data: 193).

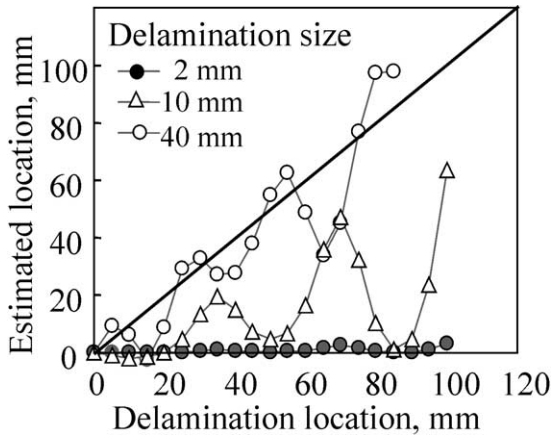

Fig. 7. Comparisons of delamination location estimations of three cases of delamination size.

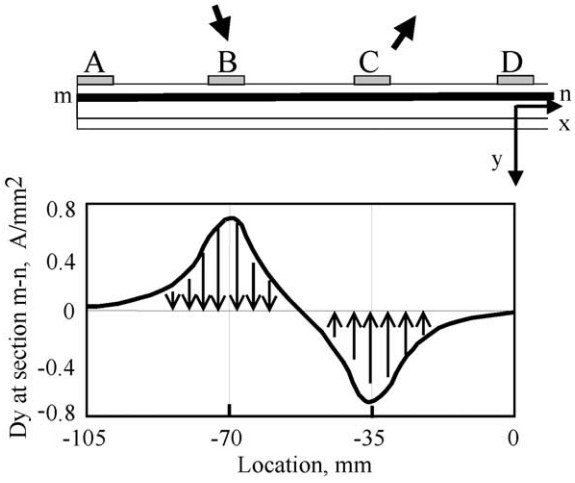

Fig. 8. Electric current density of the thickness direction at the section m–n when the specimen is charged between B and C (no delamination).

0.542 here. As shown in Fig. 5, the response surface provides poor estimations.

A response surface to estimate delamination size (length) is made from 193 data sets of FEM analyses using a quadratic polynomial. Fig. 6 shows those results. The abscissa is the given delamination size; the ordinate is the estimated delamination size. As mentioned in our previous papers [24,27], estimations of delamination size are fairly exact compared to estimations of delamination location. The adjusted coefficient of multiple-determination R^2_{adj} is 0.88 here.

To investigate the reason why the response surface of delamination location provides such poor estimations, three kinds of delamination size are plotted with different symbols in Fig. 7. In Fig. 7, the positive half side of the specimen location is plotted. The abscissa and the ordinate are identical to those of Fig. 5. Data plotted on the diagonal line indicate that estimations are absolutely exact. Symbols having large deviations from the diagonal line in the y-direction mean that the symbols have large estimation error. The figure exhibits that estimations of small delaminations of 1 mm size are very poor: almost all delamination locations are estimated to be $x = 0$ here.

On the other hand, for larger delaminations of 10 and 40 mm, estimations show periodic estimation errors. Such periodic estimation error is especially typical for delaminations of 10 mm size (triangle symbols in Fig. 7). In the case of the 10 mm delamination, local maximum estimation errors are observed in the middle of each electrode: local maximum error points are $x = 17.5$ mm, $x = 52.5$ mm, and $x = 87.5$ mm.

As mentioned in our previous paper [27], electric current in the thickness direction causes electric resistance

change. To investigate the reason for periodical estimation errors, electric current in the thickness direction is observed here. Fig. 8 shows electric current density in the thickness direction at interlamina between the top 0° ply and the middle 90° ply: the interlamina locates at the m–n line. In this figure, electric current is charged between electrodes B and C. Since another 0° ply exists in the bottom of the specimen, electric current flows through interlamina into the bottom 0° ply; electric current in the bottom 0° ply comes back to electrode C through interlamina around electrode C. This current through the interlamina makes it possible to detect a delamination, as shown in our previous paper [27]. However, as shown in Fig. 8, electric current through the interlamina is very small in the middle of the segment between electrodes B and C. This small electric current at the middle of the segment causes a slight change of electrical resistance when delamination locates at the middle of the segment.

Next, we address several cases of electrical resistances when a delamination exists at the middle of the segment; we compared them to cases in which a delamination exists just under the electrode where electric current is charged. Figs. 9–11 all depict computed electric resistance changes of cases when a delamination exists under electrode B and cases when a delamination exists at the middle of the segment between electrodes B and C. Fig. 9 shows results of a case with 2-mm delamination size. Fig. 10 shows results a case with 10 mm delamination size. Fig. 11 shows results of a case with 40 mm delamination size. In those figures, solid symbols show electric resistance changes when a delamination exists under electrode B; open symbols show electric resistance changes when a delamination exists at the middle of the segment between electrodes B and C.

In cases shown in Fig. 9 (2 mm delamination) and Fig. 10 (10 mm delamination), electric resistance change when delamination exists at the middle of the segment between electrode B and C is much smaller than those of cases when delamination exists under electrode B. Comparison of Figs. 9 and 10 reveal that shapes of electric resistance change distribution are very similar: the only difference is the respective cases' magnitude of electric resistance change.

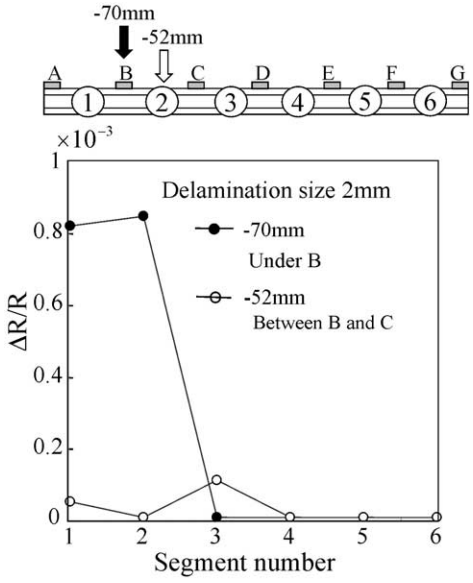

Fig. 10. Difference of electric resistance change ratio of two delamination locations when the delamination size 10 mm.

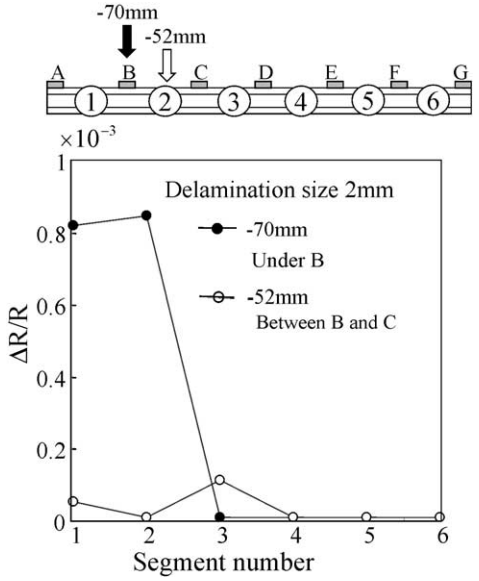

Fig. 9. Difference of electric resistance change ratio of two delamination locations when the delamination size 2 mm.

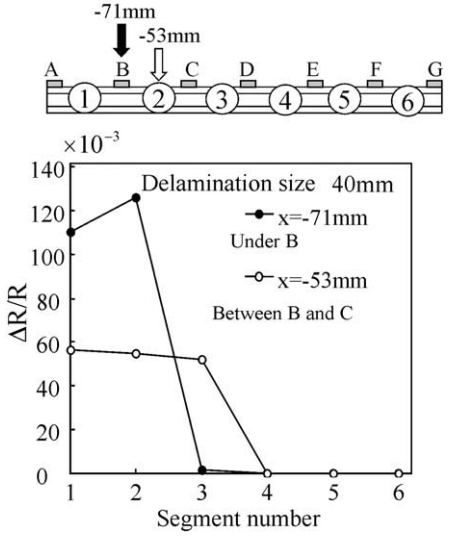

Fig. 11. Difference of electric resistance change ratio of two delamination locations when the delamination size 40 mm.

In Fig. 11 (40 mm delamination), however, electric resistance change that occurs when delamination exists at the middle of the segment is not much smaller than electric resistance change when delamination exists under electrode B. Moreover, shapes of electric resistance change of both cases differ from those in Figs. 9 and 10. That difference arises from delamination size. In the case of Fig. 11, delamination size is 40 mm, which is larger than the inter-electrode spacing (35 mm). This means that delamination cracks were partly located under an electrode even if it existed at the middle of the segment. This is inferred to be a very special case.

Fig. 9 (2 mm) and 10 (10 mm) imply that the shape of electric resistance change distribution includes information about location of delamination, but the magnitude of electric resistance change is significantly affected by both delamination size and location: when delamination exists near electrodes, electric resistance change magnitude increases; also, when a large delamination exists, electric resistance change magnitude increases. Such large differential magnitude of electrical resistance greatly complicates estimation of locations of small cracks and larger cracks that exist at the middle of the segment. Since shapes of electric resistance change distribution of Figs. 9 and 10 are quite similar to each other, we infer that standardized electrical resistance magnitude will improve estimation performance.

To verify standardization effectiveness, results of Fig. 10 (10 mm) are standardized with the magnitude of electric resistance change. The six results of electrical resistance for each segment are regarded as one of the six elements of an electric resistance change vector. Each element is divided by the square root sum of all six results as follows.

Before standardization: $(e_1, e_2, e_3, e_4, e_5, e_6)$

After standardization:

$$\left(\frac{e_1}{\delta}, \frac{e_2}{\delta}, \frac{e_3}{\delta}, \frac{e_4}{\delta}, \frac{e_5}{\delta}, \frac{e_6}{\delta}\right)\delta = \sqrt{e_1^2 + e_2^2 + e_3^2 + e_4^2 + e_5^2 + e_6^2} \tag{4}$$

Standardization results are shown in Fig. 12. In that figure, both cases' magnitudes are equally standardized. We suppose that we can distinguish the effect of delamination size and location in electric resistance changes using this standardization.

5. Application of improved method

After standardization of all electric resistance changes, new response surfaces are made from standardized data. For the response surface to estimate delamination locations, 193 sets of six standardized electric resistance changes are used. Fig. 13 shows results of estimations of delamination locations using new response surfaces. As shown in Fig. 13, the adjusted coefficient of multiple-determination R^2_{ad} is equal to 0.991. In Fig. 13, dashed lines are the error band of 10 mm. Results show that all estimations can be plotted within the error band of 10 mm: that constitutes excellent estimation of high performance for data used for regressions compared to Fig. 5. Even for small delaminations of 2 mm, estimations are excellent.

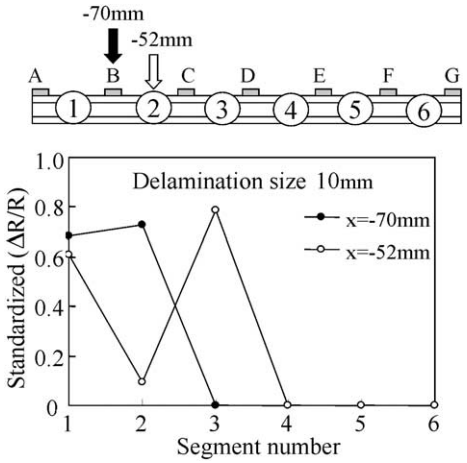

Fig. 12. Comparison of standardized electric resistance change ratio of two delamination locations when the delamination size 10 mm.

For the response surface to estimate delamination size, estimation for delamination size requires both information about location of delamination and the information of the magnitude of electric resistance changes. Since estimations of delamination locations are excellent, as shown in Fig. 13, estimated delamination location is selected as one variable for estimation of delamination size; electrical resistance magnitude δ is also selected. The total number of variables of the response surface to estimate delamination size is eight:

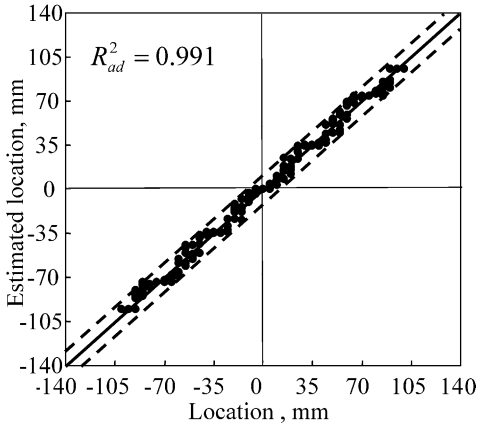

Fig. 13. Estimations of delamination location using a response surface created from standardized data (number of data: 193). Size of the delamination is from 2 to 40 mm.

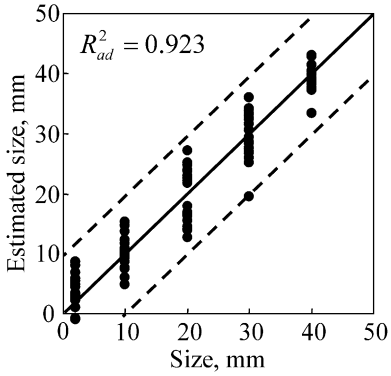

Fig. 14. Estimations of delamination size using a response surface created from standardized data and location (number of data: 193).

those are six standardized data, magnitude of electric resistance change δ and estimated delamination location in Fig. 13. Fig. 14 shows estimation results. The adjusted coefficient of multiple-determination R^2_{adj} is 0.923. The adjusted coefficient of multiple-determination R^2_{adj} is better than that of Fig. 6. Dashed lines are the 10-mm error band. Results show that all estimations can be plotted within the 10-mm error band. Estimation of delamination size is also improved through standardization.

Other variables for delamination-size estimation are possible. For example, the simplest response surface, one using only δ may be possible. When δ is adopted as the only variable (one variable) for estimation of size without using electric resistance change distribution shapes, the adjusted coefficient of multiple-determination R^2_{adj} of the response surface is 0.852. Since this value is still sufficiently high, we can conclude that the major variable for estimation of delamination size is δ (electric resistance change magnitude). When we select both δ and estimated delamination location as variables of the response surface (two variables), the adjusted coefficient of multiple-determination R^2_{adj} is 0.849. When we select six standardized electric resistance changes and δ as variables, the adjusted coefficient of multiple-determination R^2_{adj} is 0.902. Compared with Fig. 14, all of these cases provide lower adjusted coefficients of multiple-determination. Therefore, the response surface used in Fig. 14 is chosen as the best one. The δ includes information of delamination size and distance from electrodes. For large delamination cracks, distance from electrodes is unimportant (large delamination cracks have a small scatter band in Fig. 14). Distance from electrodes is very important for small delamination cracks (small delamination cracks have a large scatter band in Fig. 14). Therefore, δ is the only indicator for delamination size for large delamination cracks; delamination location is also required to determine distance from electrodes for small delamination cracks.

To investigate estimation performance for new data not used for regressions, 16 cases of delamination location and size are newly computed; then, those data are input into response surfaces to estimate delamination location and size. Results are shown in Table 2. Delamination sizes are six: 1, 5, 15, 25, 35, and 45 mm. Apparently, 1 mm and 45 mm cases are extrapolations for response surfaces because data used to make response surfaces are made from sets of data obtained using delaminations of lengths from 2 to 40 mm. However, estimations of these extrapolation cases show estimations within the error band of 10 mm as shown in Table 2. Even for 1 mm cases, estimations give good agreement with given data within the 10-mm error band. For interpolation estimations, response surfaces provide fairly exact estimations. These results lead us to conclude that response surfaces using standardized data may yield excellent high-performance estimations; also, estimation can be extrapolated within the 10-mm error band.

Table 2
Estimations and errors of new data that are not used for regressions (Unit mm)

Given delaminations		Estimated delaminations		Error of estimations	
Size	Location	Size	Location	Size	Location
1	−30	3.12	−34.57	2.12	4.57
1	68	4.48	73.76	3.48	5.76
1	7	2.83	0.00	1.83	7.00
1	−28	−2.34	−25.23	3.34	2.77
1	−10	2.80	0.00	1.80	10.00
1	73	4.48	73.76	3.48	0.76
5	78	6.40	75.55	1.40	2.45
5	−60	3.64	−66.25	1.36	6.25
5	29	5.36	34.41	0.36	5.41
5	−2	5.30	−0.22	0.30	1.78
5	−95	7.01	−95.61	2.01	0.61
5	35	6.14	34.24	1.14	0.76
15	26	11.94	34.70	3.06	8.70
15	−100	17.21	−95.82	2.21	4.18
15	12	12.96	11.12	2.04	0.88
15	−21	11.50	−25.72	3.50	4.72
15	64	15.65	72.45	0.65	8.45
15	−32	17.98	−34.77	2.98	2.77
25	−1	29.41	−0.29	4.41	0.71
25	−60	20.65	−67.43	4.35	7.43
25	22	20.98	27.61	4.02	5.61
25	43	23.30	35.79	1.70	7.21
25	−11	23.04	−8.22	1.%	2.78
25	48	17.68	45.50	7.32	2.50
25	8	25.11	3.86	0.11	4.14
35	−13	37.15	−13.81	2.15	0.81
35	−80	33.46	−76.11	1.54	3.89
35	52	28.81	51.77	6.19	0.23
35	−12	38.16	−12.01	3.16	0.01
35	0	35.58	0.00	0.58	0.00
35	30	36.01	34.37	1.01	4.37
45	−33	39.82	−34.63	5.18	1.63
45	−34	39.41	−34.99	5.59	0.99
45	−82	39.06	−75.11	5.94	6.89
45	14	46.36	14.41	1.36	0.41
45	66	40.51	67.49	4.49	1.49
45	8	39.01	9.36	5.99	1.36

6. Conclusions

To improve estimation performance of delamination location of the electric resistance change method, the present paper adopted FEM analyses of beam type specimens of various delamination size and location. An improved method was proposed here on the basis of FEM analytical results. This method was applied to estimate delamination location and size in beam type specimens. Results obtained were as follows.

1. Electric current through interlamina was very small at the middle of the segment between electrodes. This small electric current caused a small change of electric resistance when a delamination existed in the middle of the segment.
2. Standardization of electric resistance change with each magnitude of electric resistance change vector was proposed to distinguish information of delamination location and size.
3. A response surface made from standardized data gave excellent high performance estimations of delamination locations.
4. A response surface made from standardized data, magnitude of electric resistance changes and delamination location gave excellent high-performance estimations of delamination size.
5. These improved response surfaces gave good estimations for new data even for extrapolations within the error band of 10 mm.

References

[1] Moriya K, Endo T. A study on flaw detection method for CFRP composite laminates [1st report]. The measurement of Crack Extension in CFRP composites by electrical potential method. Aero and Space Sci Japan 1988;36(410):139–46 [in Japanese].

[2] Schulte K, Baron Ch. Load and failure analyses of CFRP laminates by means of electrical resistively measurements. Comp Sci Tech 1989;36:63–76.

[3] Muto N, Yanagida H, Miyayama M, Nakatsuji T, Sugita M, Ohtsuka Y. Foreseeing of Fracture in CFGFRP composites by measuring electric resistance. J Japan Soc for Comp Mat 1992; 18(4):144–50 [in Japanese].

[4] Fischer Chr, Arendts FJ. Electrical crack length measurement and the temperature dependence of the Mode I fracture toughness of carbon fibre reinforced plastics. Comp Sci Tech 1993;46:319–23.

[5] Chen PW, Chung DDL. Carbon fiber reinforced concrete for smart structures capable of non-destructive flaw detection. Smart Mater Struct 1993;2:22–30.

[6] Kaddoour AS, Al-Salehi FA, Al-Hassani STS. Electrical resistance measurement technique for detecting failure in CFRP materials at high strain rate. Comp Sci Tech 1994;51:377–85.

[7] Wolfiger C, Drechsier K. Damage detection in composite materials by monitoring electrical impedance. In Proc. of the Int. Symp. on Advanced Materials for Lightweight Structures, ESTEC, Noordwijk [ESA-WPP-070]. 1994. p. 677–782.

[8] Chen PW, Chung DDL. Carbon-fiber-reinforced concrete as intrinsically smart concrete for damage assessment during dynamic loading. J Am Ceram Soc 1995;78(3):816–8.

[9] Wang X, Chung DDL. Sensing delamination in a carbon fiber polymer-matrix composite during fatigue by electrical resistance measurement. Polymer Composites 1997;18(6):692–700.

[10] Irving PE, Thiagarajan C. Fatigue damage characterization in carbon fibre composite materials using an electric potential technique. Smart Mat Struc 1998;7:456–66.

[11] Abry JC, Bochard S, Chateauminois A, Salvia M, Giraud G. In situ detection of damage in CFRP laminates by electric resistance measurements. Comp Sci Tech 1999;59:925–35.

[12] Seo DC, Lee JJ. Damage Detection of CFRP Laminates using electrical resistance measurement and neural network. Comp Struc 1999;47:525–30.

[13] Abry JC, Choi YK, Chateuminois A, Dalloz B, Giraud G. In-situ monitoring of damage in CFRP laminates by means of AC and DC measurements. Comp Sci Tech 2001;61:855–64.

[14] Weber I, Schwartz P. Monitoring bending fatigue in carbon-fiber/epoxy composite strands: a comparison between mechanical and resistance techniques. Comp Sci Tech 2001;61:849–53.

[15] Muto N, Arai Y, Shin SG, Matsubara H, Yanagida H, Sugita M, Nakatsuji T. Hybrid composites with self-diagnosing function for preventing fatal fracture. Comp Sci Tech 2001;61:875–83.

[16] Kupke M, Schulte K, Schuler R. Non-destructive testing of FRP by DC and AC electrical method. Comp Sci Tech 2001;61: 837–47.

[17] Schueler R, Joshi SP, Schulte K. Damage detection in CFRP by electrical conductance mapping. Comp Sci Tech 2001;61: 921–30.

[18] Kubo S, Kuchinishi M, Sakagami T, Ioka S. Identification of delamination in layered composite materials by the electric potential CT method, applied electromagnetics and mechanics. In: Takagi T, Uesaka M, editors. Proc. of the 10th Int. Symp. on Applied Electromagnetics and Mechanics, Japan Soc. Appl Electromag and Mech. 2001. p. 641–2.

[19] Todoroki A, Matsuura K, Kobayashi H. Application of electric potential method to smart composite structures for detecting delamination. JSME Intl J, Series A 1995;38(4):524–30.

[20] Todoroki A, Kobayashi H, Matsuura K. Application of electrical potential method as delamination sensor for smart structures of graphite/epoxy. In: Inoue K, Shen SIY, Taya M, editors. US–Japan Workshop on Smart Materials and Structures. University of Washington TMS; 1997. p. 47–54.

[21] Todoroki A. Delamination detection by electric resistance change for graphite/PEEK Composites. Proceedings of the 5th Japan International SAMPE Symposium 1997:899–904.

[22] Todoroki A, Suzuki H, Kobayashi H, Nakamura H, Shimamura Y. Evaluation of orthotropic electrical resistance for delamination detection of CFRP by electrical potential method. Trans Japan Soc of Mech Engnrs Series A 1998;64(622):1654–9 [in Japanese].

[23] Todoroki A, Suzuki H. Health Monitoring of internal delamination cracks for Graphite/epoxy composites by electric potential method. Appl Mech Engng 2000;5(1):283–94.

[24] Todoroki A, Tanaka Y, Shimamura Y. Response surface for delamination monitoring of graphite/epoxy composite using electric resistance change. In: Chang FK, editor. Structural Health Monitoring 2000. Technomic; 1999. p. 308–16.

[25] Todoroki A, Tanaka Y, Shimamura Y. Electric resistance change method for identification of embedded delamination of CFRP plates materials science research international, special technical publication-2. JSMS 2001:139–45.

[26] Todoroki A, Tanaka Y, Shimamura Y. Delamination monitoring of graphite/epoxy laminated composite plate of electric resistance change method. Comp Sci Tech 2002;62(5):629–39.

[27] Todoroki A, Tanaka M, Shimamura Y. Measurement of orthotropic

electric conductance of CFRP laminates and analysis of the effect on delamination monitoring with electric resistance change method. Comp Sci Tech 2002;62(5):619–28.

[28] Todoroki A. Effect of number of electrodes and diagnostic tool for delamination monitoring of graphite/epoxy laminates using electric resistance change. Comp Sci Tech 2001;61(13): 1871–80.

[29] Myers R, Montgomery DC. Response surface methodology process and product optimization using designed experiments. 2nd ed. New York: Wiley Inter-science Publication; 2002.